

**Infrared spectroscopy study of structural changes in glass-forming salol**J. Baran<sup>1</sup> and N. A. Davydova<sup>2</sup><sup>1</sup>*Institute of Low Temperature and Structure Research, PAS, 50-950 Wrocław, Poland*<sup>2</sup>*Institute of Physics, NANU, 46, pr. Nauki, 03028 Kiev, Ukraine*

(Received 1 December 2009; published 12 March 2010)

We report the investigation of glass-forming salol upon different courses of the temperature changes from liquid to glass state and back using FT-IR spectroscopy measurements in the wide spectral and temperature ranges. The formation of the ordered clusters in supercooled liquid salol has been observed at 250 K. When the temperature is decreased further to 11 K these ordered clusters become an element of the glass structure. With increasing temperature to 270 K through the glass transition noticeable evolutions of the IR spectrum occurs up till the ordered clusters are developed into crystal. So produced crystal melts in the temperature range 300–310 K, that corresponds to the melting temperature of the metastable phase ( $T_{\text{melt}}=302$  K). Thus, the crystalline structure of the ordered clusters corresponds to the structure of metastable phase and is monoclinic.

DOI: [10.1103/PhysRevE.81.031503](https://doi.org/10.1103/PhysRevE.81.031503)

PACS number(s): 64.70.P-, 61.43.Fs, 64.60.My, 78.30.-j

**I. INTRODUCTION**

Experiments on glass-forming liquids reveal a pronounced slowdown of their dynamics that accompanies supercooling, which can be rationalized in term of the picture of dynamical heterogeneities [1–5]. The Adam–Gibbs theory explained the temperature dependence of relaxation behavior in glass forming liquids in terms of the temperature variation of the size of “cooperatively rearranging regions” [6]. Stillinger and Hodgdon [7] have proposed a “fluidized domain” model where the supercooled liquid is pictured essentially as a solid glass with small fraction of domains. Cohen and Grest have worked out a two-phase model where “liquidlike cells” are aggregated into liquidlike clusters that percolate into the critical cluster [8]. Kivelson *et al.* [9,10] have developed a theory where “frustrated-limited domains” are formed as a liquid is cooled below an avoided critical point. An alternative model has been proposed by Tanaka [11,12], which is based on the idea that in any liquid there always exist two competing ordering, which lead to two types of local structures frustrated with each other: (i) normal-liquid structures and (ii) locally favored structures. However, the structure of cooperatively rearranging regions, frustrated-limited domains, or locally favored structures is far from being completely understood.

Eckstein *et al.* [13] reported the pronounced changes in the liquid structure of two glass-forming liquids, salol, and propylene carbonate as a function of temperature on the bases of the wide angle x-ray measurements. The authors of [13] have observed that at high temperatures the scattering line shape shows one mainly symmetric diffraction peak ( $q_{\text{max}} \sim 1.38 \text{ \AA}^{-1}$ ). It changes its shape as the temperature decreases; developing a peak at  $q$  higher than the  $q_{\text{max}}$  and is becoming increasingly asymmetric. Such behavior of the x-ray intensities is interpreted in terms of clusterlike heterogeneities forming in the liquid as  $T_g$  is approach. This interpretation was based on the heterogeneous liquid model proposed by Fisher *et al.* [14]. (For more details see [13]). Open question remains concerning the structure of these clusters. Are they “glassy,” “nonperiodic solids,” or ordered clusters? Eckstein *et al.* for calculation of the scattering intensities

considered the clusterlike heterogeneities as crystalline clusters composed of phenyl-benzoate molecules.

Recently we have found for benzophenone and 2-biphenylmethanol that in their supercooled liquids the metastable nuclei start to appear near  $T_g$  [15–17]. Moreover their structure is not consistent with that of the initial crystal. The nuclei, which composed of about 1000 molecules can be recognized as a kind of cluster with ordered structure. The formation of the crystalline nuclei within a supercooled liquid state near  $T_g$  should not be unique to benzophenone and 2-biphenylmethanol, but on our opinion may also take place in salol. Namely, we suggest that a supercooled liquid salol near  $T_g$  is in a dynamically heterogeneous state composed of the fluctuating nuclei (ordered clusters), which may be the origin of so-called prepeak, which is observed in the high  $q$  side of the main peak  $S(q)$  [13].

In order to verify this suggestion we have performed infrared spectroscopy study, which is known as a powerful tool for the nondestructive structural information of thin films. We will focus on a careful study of the Fourier-transform infrared (FT-IR) spectra upon different courses of the temperature changes from a liquid to glass state and back. The easily accessible melting point ( $T=315$  K) and glass transition temperature ( $T_g=223$  K) provides a convenient temperature range where the supercooled liquid state of salol can be studied by means of IR spectroscopy.

**II. EXPERIMENT**

Salol [phenyl salicylate or phenyl-2-hydroxybenzoate; 2-(OH)C<sub>6</sub>H<sub>4</sub>CO<sub>2</sub>C<sub>6</sub>H<sub>5</sub>] of 99% purity was purchased from Aldrich. Salol was used without further purification. Its chemical structure is shown in Fig. 1. The molecule is asymmetric one consisting of two phenyl rings, which are connected by three single bonds. The hydroxyl (OH) and carbonyl (C=O) groups are involved in the formation of an intramolecular hydrogen bonding. Also salol is known to demonstrate two crystalline morphologies, metastable (monoclinic) and stable (orthorhombic) phases, with respective melting points of 302 and 315 K [18,19]. The metastable phase is unstable and readily undergoes a heavily displacive

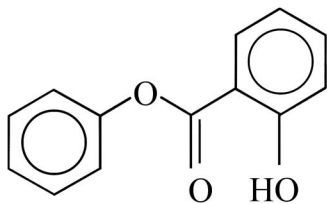


FIG. 1. Chemical structure of salol.

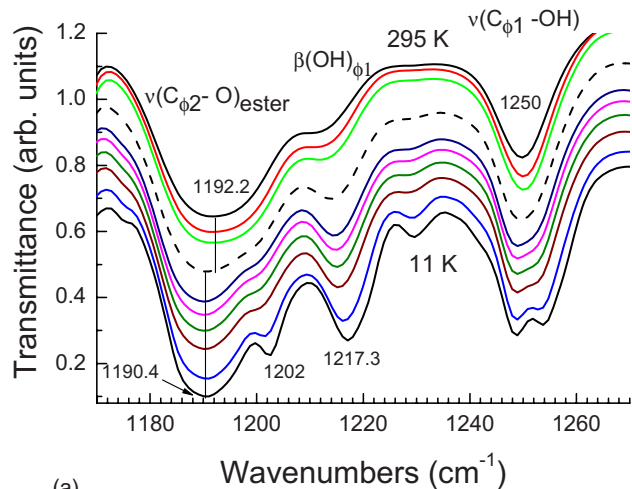
monotropic transition to the stable phase. This transformation can occur spontaneously [19].

Infrared measurements were done on a Fourier-transform infrared spectrometer (Bruker model IFS-88) at a resolution  $2\text{ cm}^{-1}$  and 32 scans were typically co-added for an individual spectrum. Data processing was performed with OPUS software. For the infrared (IR) measurements, a sample of powder salol was inserted in a cell with two CsI pellets at room temperature, and then melted into thin film. The thickness of such a cell was approximately a few micrometers. Such sample with liquid salol was then fixed in a closed-cycle cryostat providing a temperature variation in the range 330–11 K. In the region between the glass transition temperature and melting point salol exhibits an enhanced crystallization tendency and some effort is needed to prevent it from crystallization.

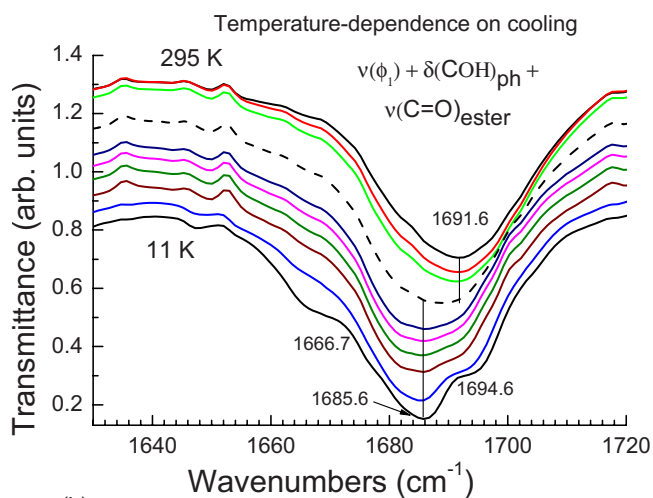
### III. RESULTS

IR experiments have only been carried out on salol crystal at room temperature so far [20]. Also, quantum-chemical calculations of vibrational frequencies for the normal modes of salol molecule have been performed [20]. We have studied FT-IR spectra absorption in the  $400\text{--}4000\text{ cm}^{-1}$  spectral range. 77 active fundamental modes of salol molecule are expected in the calculated IR spectrum [20], but we observed more than 90 bands in the experimental spectrum of salol crystal at low temperature. However, in this paper, we focus only on those vibrations, which are most significantly affected by intra and intermolecular hydrogen-bonding. The maximal influence of the structural changes should be expected for the vibration frequencies that involve hydroxyl and carbonyl groups. These include  $\nu(\text{C}_{\phi_1}\text{-OH})_{\text{ph}}$  and  $\nu(\text{C}=\text{O})$  stretching vibrations,  $\delta(\text{C-OH})_{\text{ph}}$  and  $\beta(\text{OH})_{\phi_1}$  in-plane bending vibrations in the phenyl hydroxyl group. All assignments of the normal vibrations are those as in [20].

Figures 2(a) and 2(b) show fragments of the IR absorption spectra of salol recorded on cooling from the room temperature down to 11 K in the  $1170\text{--}1270\text{ cm}^{-1}$  and  $1630\text{--}1730\text{ cm}^{-1}$  spectral regions, respectively. The curves are vertically shifted for the sake of clarity. In the  $1170\text{--}1270\text{ cm}^{-1}$  region, two bands centered at  $1192.2\text{ cm}^{-1}$  and at  $1250.0\text{ cm}^{-1}$  dominate the spectra at room temperature [Fig. 2(a)], which are ascribed to the  $\nu(\text{C}_{\phi_2}\text{-O})_{\text{ester}}$  and  $\nu(\text{C}_{\phi_1}\text{-OH})_{\text{ph}}$  stretching vibrations, respectively [20]. It is seen that with the temperature decreasing from 295 to 260 K the spectra are essentially unchanged [Fig. 2(a)]. At the temperatures of 250 K (dashed curve) and 240 K the change of the spectra is clearly seen. The band at



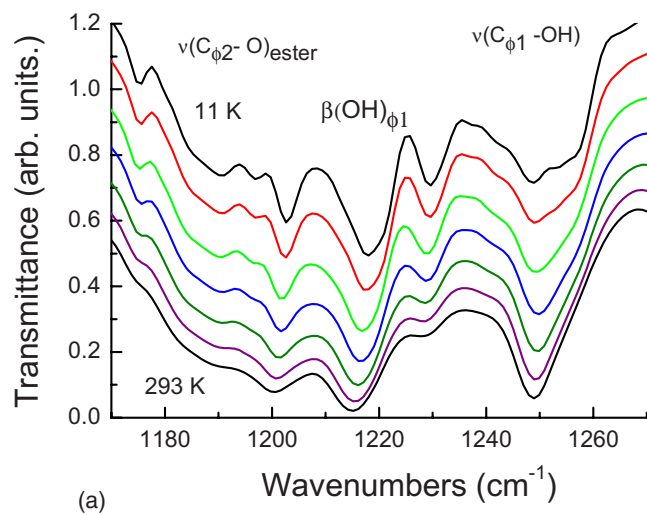
(a)



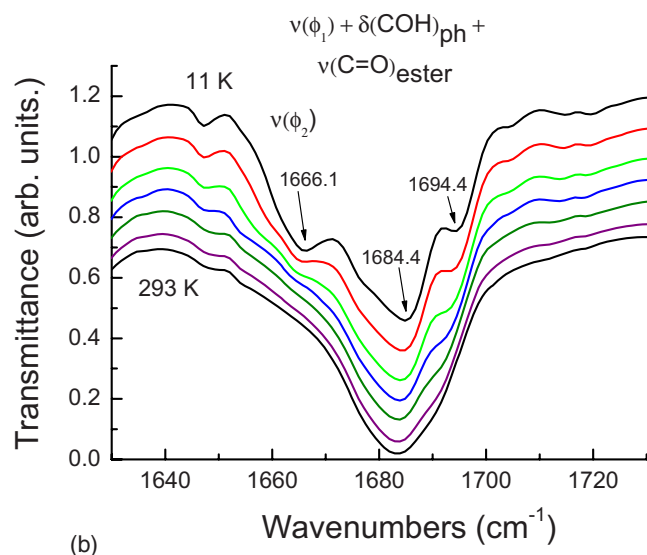
(b)

FIG. 2. (Color online) Temperature-dependent IR spectra variations for salol in the  $1170\text{--}1270$  (a) and  $1630\text{--}1730\text{ cm}^{-1}$  (b) spectral regions recorded on cooling. Temperatures are (top to bottom): 295, 270, 260, 250 (dashed), 240, 230, 210, 190, 110, and 11 K. The curves are shifted for clarity.

$1192.2\text{ cm}^{-1}$  is shifted by  $1.8\text{ cm}^{-1}$  to the low-frequency side. When the temperature decreases further down to 11 K the position of the band at  $1190.4\text{ cm}^{-1}$  stays almost constant. The band at  $1215\text{ cm}^{-1}$  ascribed to the  $\beta(\text{OH})_{\phi_1}$  bending vibration sharply increases in the intensity and its position moves to higher frequencies. Also at low temperatures the splitting of the band at  $1250\text{ cm}^{-1}$  into two components is observed. As can be seen from Fig. 2(b), in the  $1630\text{--}1730\text{ cm}^{-1}$  spectral region a broad band centered at  $1691.6\text{ cm}^{-1}$  characteristic of the  $\nu(\text{C}=\text{O})$  stretching vibrations dominates. As shown in [20] this band originates from the combination of the  $\nu(\text{C}_{\phi_1})$  stretching and  $\delta(\text{COH})_{\text{ph}}$  bending modes. Lowering the temperature also leads to the transformation of the spectra, which is clearly observed in the  $250\text{--}240\text{ K}$  temperature region. The dominant band at  $1691.6\text{ cm}^{-1}$  shifts to lower frequencies (to  $1685.6\text{ cm}^{-1}$ ). When the temperature decreases further to 11 K, its position



(a)

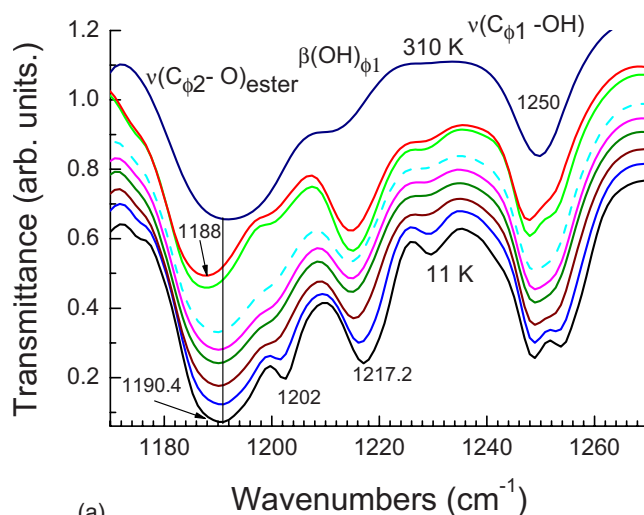


(b)

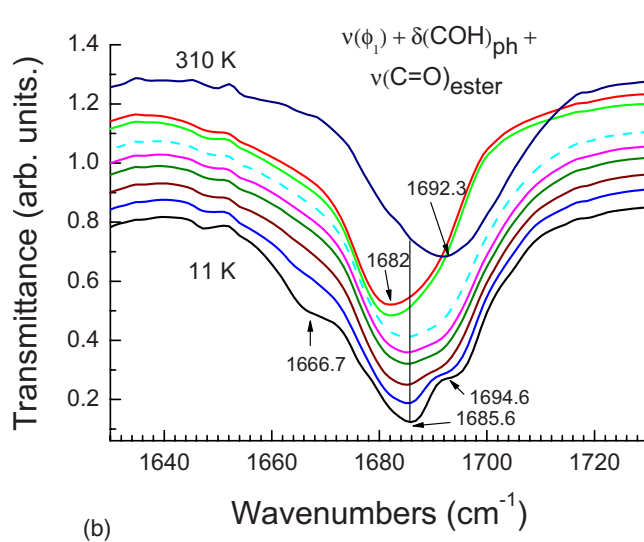
FIG. 3. (Color online) Temperature-dependent IR spectra for crystalline salol in the 1170–1270 (a) and 1630–1730  $\text{cm}^{-1}$  (b) spectral regions. The temperatures are (top to bottom): 11, 70, 110, 150, 190, 230, and 293 K. The curves are shifted for clarity.

practically does not change, however two additional bands at  $1666.7 \text{ cm}^{-1}$  and at  $1694.6 \text{ cm}^{-1}$  are starting to emerge. The first one corresponds to  $\nu(\phi_2)$  stretching vibration.

For comparison the temperature-dependent IR spectra of crystalline salol are shown in Figs. 3(a) and 3(b). In the 1170–1270  $\text{cm}^{-1}$  region the spectra are dominated by a band at  $1218 \text{ cm}^{-1}$  ascribed to the  $\beta(\text{OH})_{\phi_1}$  in-plane bending vibrations, with other bands present at  $1174.6$ ,  $1190.5$ ,  $1196.7$ ,  $1202.6$ ,  $1229.5$ ,  $1249.0$ , and  $1254.3 \text{ cm}^{-1}$  [Fig. 3(a)]. With decreasing temperature the smooth changes in the shape as well as in the positions of these bands are observed. In the  $1630\text{--}1730 \text{ cm}^{-1}$  region [Fig. 3(b)] the dominant band at  $1684.4 \text{ cm}^{-1}$  practically does not change its position with decreasing temperature. However, the shape of this band gradually changes with decreasing temperature, and fi-



(a)



(b)

FIG. 4. (Color online) Temperature-dependent IR spectra variations for salol in the 1170–1270 (a) and 1630–1730  $\text{cm}^{-1}$  (b) spectral regions recorded on heating. Temperatures are (bottom to top): 11, 110, 190, 210, 230, 250 (dashed), 270, 300, and 310 K. The curves are shifted for clarity.

nally, two bands at  $1666.1$  and  $1694.4 \text{ cm}^{-1}$  appear and grow in the intensity as 11 K is approach.

Figures 4(a) and 4(b) show the fragments of the IR spectra recorded upon heating the glassy state from 11 to 310 K. The temperature changes from bottom to top. It is seen from Fig. 4(a), that the shape of the band at  $1190.4 \text{ cm}^{-1}$  and its position does not change with increasing temperature from 11 to 230 K. Moreover, the behavior of the spectra in the both spectral regions (Fig. 4) is almost identical to those recorded on cooling from 230 to 11 K (Fig. 2). At 250 K (dashed curve) only small changes of the spectrum are seen, whereas the changes become more prominent with temperature increasing up to 270 (Fig. 4). The bands at  $1190.4 \text{ cm}^{-1}$  [Fig. 4(a)] and at  $1685.6 \text{ cm}^{-1}$  [Fig. 4(b)] do significantly shift toward the lower frequency. Also it is seen that at 250 K this band (dashed curve) is much wider compared to that at

270 K. The temperature increasing to 300 K does not lead to the changes between the spectra recorded at 270 and 300 K. Such transformation of the spectra upon heating can be related to the crystallization of the sample at 270 K. A slight increase of the temperature from 300 to 310 K leads to sharply defined changes in the both regions of the spectra (Fig. 4). The studied bands become again weaker and wider. Also a drastic increase in the frequency of the stretching modes  $\nu(C_{\phi 1}-OH)_{ph}$  and  $\nu(C=O)$  is seen. The spectrum recorded at 310 K (Fig. 4) coincides with the spectrum of liquid salol recorded at 295 K (Fig. 2). This coincidence is an evidence of the melting of the crystalline phase in the temperature range of 300–310 K. Moreover, the fact that the melting temperature lies below 310 K suggests that we are dealing with the metastable phase of salol that melts at 302 K according to [18,19]. The stable phase of salol melts at 315 K. This conclusion is further supported by the comparison of the IR spectra of the so produced metastable phase and the stable phase of salol.

In Figs. 5(a) and 5(b) we compare the room-temperature IR spectra of liquid, metastable and stable phases of salol. To initiate the crystallization of the stable phase, the crystalline powder of the stable phase was added to the edge of the cell containing a liquid thin film of salol. It is seen from the figure that the IR spectra obtained are markedly different in the both spectral regions. The intensity of the band at 1188.0  $cm^{-1}$  in the metastable phase spectrum is stronger as compared to that in the stable phase, while the bands at 1199.6 and 1215.0  $cm^{-1}$  are weaker [Fig. 5(a)]. In the 1630–1730  $cm^{-1}$  spectral region [Fig. 5(b)], the position of the  $\nu(C=O)$  band in the stable (1683.3  $cm^{-1}$ ) and metastable (1682.0  $cm^{-1}$ ) phase is shifted correspondingly by 8.9 and 10.2  $cm^{-1}$  compared to its position in the liquid phase spectrum. The differences between the IR spectra of salol crystallized as the room temperature was approaching from below, and its stable phase, do support our suggestion concerning the metastable phase formation in the supercooled liquid.

#### IV. DISCUSSION

We will discuss our results in the context of the metastable nuclei formation in supercooled liquid salol. It is well known that the nucleation is a process connected with the overcoming of a free-energy barrier in order to form and then grow into the new phase. The transformation of one phase from another by growth of the nuclei forming randomly in the parent phase is described by the Avrami equation. It can specifically describe the kinetics of crystallization. Unfortunately, using IR spectroscopy we have no way of studying the crystallization kinetics.

Our results show that on cooling liquid salol from room temperature (Fig. 2) below 250 K the crystalline nuclei appear and disappear until their size reaches some critical value above which the nuclei are thermodynamically stable. They can be recognized as nanoclusters comprising ordered molecules. At low temperatures a crystal growth is suppressed because the rearrangement of molecules is frozen kinetically, thus, a liquid vitrifies at  $T_g=223$  K without crystallization.

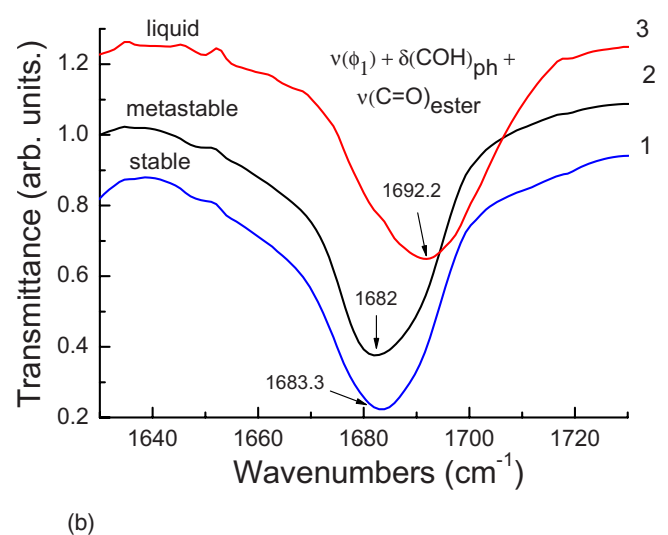
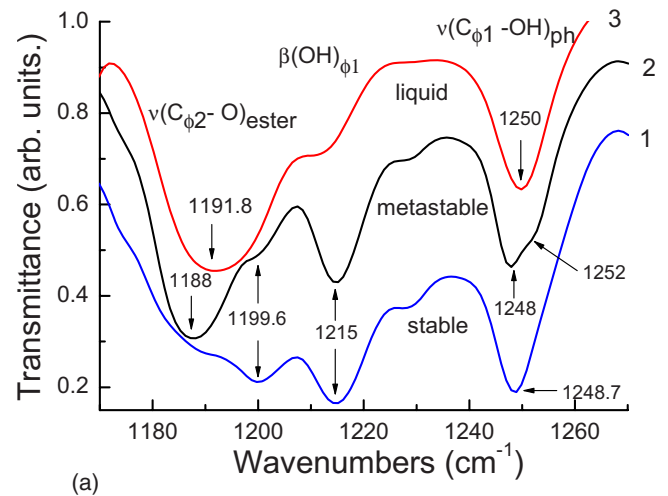


FIG. 5. (Color online) IR spectra of salol at  $T=295$  K in the 1170–1270 (a) and 1630–1730  $cm^{-1}$  (b) spectral regions: (1)—liquid film, (2)—metastable phase (after cooling followed by heating); (3)—crystalline film of the initial sample.

The nanometric scale ordered clusters become an important element of the glass structure.

The IR spectra of salol recorded upon cooling from room temperature to 230 K coincide with those recorded upon heating from 11 to 230 K. This is clearly seen from Fig. 6(a), where we compare the spectra recorded at 230 K. With increasing the temperature through the glass transition temperature, the molecules can change their positions or orientations, so the ordered clusters get a possibility to grow. Thus, we should expect that the IR spectra recorded on cooling should differ from those recorded on heating at the same temperature point. Moreover, this difference between the spectra should increase with the temperature increasing, indicating on the changes in the liquid structure. The small discrepancies are seen between the spectra recorded at 250 K [Fig. 6(b)]; however the differences between the spectra recorded at 270 K become drastic [Fig. 6(c)]. In the last case,

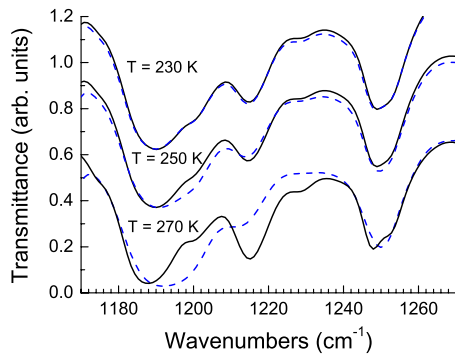


FIG. 6. (Color online) IR spectra of salol in the 1170–1270  $\text{cm}^{-1}$  spectral region at  $T=230$  K (a), 250 K (b), and 270 K (c): (solid curves) the spectra recorded on heating; (dashed curves) the spectra recorded on cooling.

when we approach the 270 K point from room temperature, we have to deal with an original liquid (dashed curve), but when we approach this point from the glassy state, the nuclei already exist and have a possibility to grow that results in the crystallization (solid curve).

As has been shown above, the IR spectra of the metastable and stable phases of salol are quite different (Fig. 5), which is due to different packing of the molecules in these two phases. It is also interesting to note that the density of the metastable phase is lower than that of the stable one [19]. As was mentioned above, a formation of clusterlike heterogeneities was proposed in [13] as an explanation for the pronounced changes in the liquid structure of salol. In the present paper we have shown that the observed changes in the IR spectra of salol could be reasonably explained by the formation of ordered clusters (nuclei), having the structure of salol metastable phase. From this it is natural to conclude that namely the metastable ordered clusters are responsible for the so-called prepeak observed in x-ray measurements [13]. The authors of [13] were able to explain the characteristic changes of the  $S(q)$  line shape by the scattering intensities calculated for crystalline spherical clusters of phenylbenzoate molecules. These clusters in some sense bear close similarity to the crystalline clusters composed of salol molecules packed into the metastable phase observed in the present paper. However, in the heterogeneous liquid model [14], which was used for the explanation of the x-ray experimental data [13], the heterophase fluctuations have been considered to be completely independent of the nucleation process.

In our opinion, the formation of the crystalline nuclei within a supercooled liquid is not peculiar to a certain sub-

stance, and could be a universal phenomenon. The examples in support of the nucleation in supercooled liquid are the observation of a “glacial” state in triphenyl phosphite [21–24] and  $n$  butanol [25,26]. The new solid phase originating from supercooled liquid and denoted as the “glassial” phase was first observed in triphenyl phosphite by Kivelson and co-workers [21]. A number of conjectures have been proposed concerning the structure of the glacial phase, and most of them describe the phase as a poorly crystallized defect-ordered phase [21–24]. Some groups proposed to explain its origin as a second amorphous state [27], others as a plastic-crystal state [28]. In the recent papers [25,26] by different experimental techniques it has been convincingly demonstrated for  $n$  butanol, that the “glacial” state is not an amorphous phase, but is composed of crystallites of the stable phase coexisting with an untransformed supercooled liquid. Recently, the nucleation-growth-type transformation for  $n$  butanol has been directly observed with optical microscopy [29]. Also the formation of nuclei has been suggested to form in the early stage of polymer crystallization [30]. Recent computer simulation study [31] concerning the relationship between the dynamics and the medium range crystalline structure shows that dynamic heterogeneity and the slow dynamics are intrinsically related to the medium-range crystalline ordering in a supercooled liquid. In the theoretical paper [32], it was shown that the introduction of the parameter  $\varphi$  equal to the specific volume occupied by the nuclei of the solid state provides a natural explanation of the temperature dependence of the density and thermal expansion coefficients of glycerol in its liquid, solid amorphous, glassy, and crystal states.

## V. CONCLUSION

In this paper, we have investigated glass-forming salol using IR spectroscopy. The most important results of this paper are the observation of the formation of the ordered clusters (nuclei) at 250 K in the supercooled salol and their development at 270 K as this temperature is approach from glassy state. The growth of the ordered clusters leads to crystallization into the metastable phase of salol.

The performed investigations of salol allow us to answer the question concerning the structure of clusterlike heterogeneities proposed by E. Eckstein *et al.* [13] as an explanation for the x-ray intensities. Namely, we can state that these clusterlike heterogeneities are ordered clusters with the structure, which corresponds to that of the metastable phase of salol.

[1] E. W. Fischer, *Physica A* **201**, 183 (1993).  
 [2] H. Sillescu, *J. Non-Cryst. Solids* **243**, 81 (1999).  
 [3] M. D. Ediger, *Annu. Rev. Phys. Chem.* **51**, 99 (2000).  
 [4] R. Richert, *J. Phys.: Condens. Matter* **14**, R703 (2002).  
 [5] J. D. Stevenson, J. Schmalian, and P. G. Wolynes, *Nat. Phys.* **2**, 268 (2006).

[6] G. Adam and I. H. Gibbs, *J. Chem. Phys.* **43**, 139 (1965).  
 [7] F. H. Stillinger and J. A. Hodgdon, *Phys. Rev. E* **53**, 2995 (1996).  
 [8] M. H. Cohen and G. S. Grest, *Phys. Rev. B* **20**, 1077 (1979).  
 [9] C. A. Angel, *J. Non-Cryst. Solids* **354**, 4703 (2008).  
 [10] D. Kivelson and G. Tarjus, *J. Non-Cryst. Solids* **235-237**, 86

- (1998).
- [11] H. Tanaka, *J. Phys.: Condens. Matter* **11**, L159 (1999).
- [12] H. Tanaka, *J. Non-Cryst. Solids* **351**, 3385 (2005).
- [13] E. Eckstein, J. Qian, R. Hentschke, T. Thurn-Albrecht, W. Steffen, and E. Fischer, *J. Chem. Phys.* **113**, 4751 (2000).
- [14] E. W. Fischer and A. S. Bakai, in *Heterophase Fluctuations in Supercooled Liquids and Polymers*, AIP Conference Proceedings No. 469, edited by M. Tokuyama and I. Oppenheim (AIP, Melville, NY, 1999), p. 325–338.
- [15] N. A. Davydova, V. I. Mel'nik, J. Baran, and M. Drozd, *J. Mol. Struct.* **651-653**, 171 (2003).
- [16] N. A. Davydova, V. I. Mel'nik, K. I. Nelipovitch, J. Baran, and J. I. Kukielski, *Phys. Rev. B* **65**, 094201 (2002).
- [17] J. Baran, N. A. Davydova, M. Drozd, and A. Pietraszko, *J. Phys.: Condens. Matter* **18**, 5695 (2006).
- [18] J. H. Bilgram, U. Doring, M. Wachter, and P. Seiler, *J. Cryst. Growth* **57**, 1 (1982).
- [19] R. B. Hammond, M. J. Jones, K. J. Roberts, H. Kutzke, and H. Klapper, *Z. Kristallogr.* **217**, 484 (2002).
- [20] J. Hanuza, W. Sasiadek, J. Michalski, J. Lorenc, M. Maczka, A. A. Kaminski, A. V. Butashin, H. Klapper, J. Hulliger, and Abudelrhman F. A. Mohmed, *Vib. Spectrosc.* **34**, 253 (2004).
- [21] A. Ha, I. Cohen, X. Zhao, M. Lee, and D. Kivelson, *J. Chem. Phys.* **100**, 1 (1996).
- [22] G. Tarjus, C. Alba-Simionesco, M. Grousson, P. Viot, and D. Kivelson, *J. Phys.: Condens. Matter* **15**, S1077 (2003).
- [23] A. Hedoux, Y. Guinet, and M. Descamps, *Phys. Rev. B* **58**, 31 (1998).
- [24] A. Hedoux, Y. Guinet, P. Derollez, O. Hernandez, L. Pacon, and M. Descamps, *J. Non-Cryst. Solids* **325**, 4984 (2006).
- [25] A. Wypych, Y. Guinet, and A. Hedoux, *Phys. Rev. B* **76**, 144202 (2007).
- [26] M. Hassaine, R. J. Jimenez-Rioboo, I. V. Sharapova, O. A. Korolyuk, A. I. Krivchikov, and M. A. Ramos, *J. Chem. Phys.* **131**, 174508 (2009).
- [27] Ch. Alba-Simionesco and G. Tarjus, *Europhys. Lett.* **52**, 297 (2000).
- [28] G. P. Johari and C. Ferrari, *J. Phys. Chem. B* **101**, 10191 (1997).
- [29] R. Kurita and H. Tanaka, *J. Phys.: Condens. Matter* **17**, L293 (2005).
- [30] M.-K. Hsieh and S.-T. Lin, *J. Phys.: Condens. Matter* **21**, 505101 (2009).
- [31] H. Shintani and H. Tanaka, *Nat. Phys.* **2**, 200 (2006).
- [32] I. V. Blazhnov, N. P. Malomuzh, and S. V. Lishchuk, *J. Chem. Phys.* **121**, 6435 (2004).